

Atomistically-Informed Continuum Model for Hydrogen Storage on Graphene

by Feng Shi, Amar Bhalla, Chonglin Chen, Gemunu H. Gunaratne, Jiechao Jiang, and Efstathios I. Meletis

Hydrogen is considered to be a possible “clean energy” solution and the associated problem of hydrogen storage (and retrieval on demand) has seen intense activity in recent years. Carbon-based storage materials in general and graphene¹⁻⁴ in particular have attracted much attention due to their efficient hydrogen sorption capabilities. While some of the early works focused on pristine graphene, decorated graphene (usually with metal atoms) appears to show significant promise in terms of storage capacity albeit at the cost of complications of fabrication and stability.⁵ Most of the interesting insights into the mechanisms of hydrogen storage and interpretations of experiments on undecorated and decorated graphene are based on atomistic calculations—either first-principles based or predicated on empirical force fields. For example, some early questions like, why does molecular H₂ chemisorption occur on graphene despite the fact that molecular binding energy is 2.4 eV in contrast to the relatively weaker 0.8 eV binding energy of hydrogen to graphene were addressed through first principles calculations.⁶

Atomistic methods, while providing (if used properly) accurate insights, are limited in both spatial and temporal scales they can access. For example, pressure-temperature-concentration evolution of the hydrogenation process is inaccessible by any of the atomistic methods. The latter are precisely the parameters required to guide experiments. In this brief note, we propose a phenomenological continuum model that readily connects to parameters (such as binding energies) available from atomistic calculations and provides a first order computation of the dynamics of hydrogen adsorption on graphene. While we focus on pristine graphene, the presented framework can be modified to account for decorated graphene as well as incorporate other subtleties such as impurities, significant elastic deformations among others. As example, a prediction of considerable experimental interest, we present results for the maximum concentration that can be achieved for given initial pressure.

The Model and Results

We consider an extended (perfect) graphene sheet placed in a fixed amount of H₂ gas. We consider the absorption and desorption of H₂. We show first that computations of energy reported in Ref. 6 for absorption of small clusters of hydrogen are consistent with a model whose energy depends on two terms: (1) an on-site contribution, and (2) a nearest neighbor contribution. We use a continuum analog of the resulting Ising model to deduce the free energy for the system.

The total free energy G of the system is the sum of G_{H_2} and G_g , which are the free energies of the hydrogen gas and the hydrogenated graphene sheet respectively.

$$G = G_{H_2} + G_g \quad (1)$$

The hydrogen gas is regarded as ideal gas, and hence its Gibbs free energy is⁷

$$G_{H_2} = U_{H_2} + PV - TS_{H_2} \quad (2)$$

where U_{H_2} is its internal energy, and S_{H_2} is the entropy of the hydrogen gas.

The internal energy is

$$U_{H_2} = c_v n k_B T \quad (3)$$

where c_v is the heat capacity at a constant volume, n is the number of the hydrogen molecules, k_B is the Boltzmann constant. S_{H_2} is given by⁷

$$S_{H_2} = k_B \ln(Z_{trans} \cdot Z_{rot}) + k_B T \left(\frac{\partial \ln(Z_{trans} \cdot Z_{rot})}{\partial T} \right) \quad (4)$$

Where Z_{trans} and Z_{rot} are the translational the rotation contribution to the partition function. Substituting:

$$Z_{trans} = \frac{1}{n!} \left[\frac{(2\pi m k_B T)^{3/2} V}{h^3} \right]^n, \text{ and } Z_{rot} = \left(\frac{8\pi^2 I k_B T}{\sigma h^2} \right) \text{ into Eq. 2, we}$$

find that

$$\begin{aligned} S_{H_2} &= k_B n \left(\underbrace{\frac{3}{2} \ln \frac{2\pi m k_B T}{h^2} + \ln \frac{V}{n} + \frac{5}{2}}_{S_{trans}} + \underbrace{\ln \frac{8\pi^2 I k_B T}{\sigma h^2} + 1}_{S_{rot}} \right) \\ &= k_B n \left(\underbrace{\ln \frac{8\pi^2 I k_B (2\pi m k_B)^{3/2}}{\sigma h^{69.22}} + \frac{7}{2}}_{S_{trans}} + \ln T^2 + \ln \frac{V}{n} \right) \end{aligned} \quad (5)$$

where $m = 1.66 \times 10^{-24}$ kg is the mass of a hydrogen molecule, $I = 4.72 \times 10^{-48}$ kg is the moment of inertia of a hydrogen molecule, h is the Planck constant.

Free energy of the graphene sheet is given by

$$G_g = E_g - TS_g \quad (6)$$

The process of the hydrogenation can be analyzed using

$$E_g + \frac{n_1}{2} \varepsilon_H \rightarrow E_{H@g} + n_1 \varepsilon_b \quad (7)$$

where E_g is the internal energy of the graphene with no H attached, $\varepsilon_H = 2.3$ eV is the binding energy of the hydrogen gas, and ε_b is the mean binding energy of the hydrogenation.

Rescaling Eq. 7 and setting $E_s = 0$

$$E_{H@g} = n_1 (\varepsilon_H - \varepsilon_b) \quad (8)$$

Combining Eq.1, Eq. 6, and Eq. 8, we find that

$$G = G_{H_2} \Big|_{n=n_0-n_1} + n_1 (\varepsilon_H - \varepsilon_b) - TS_g \quad (9)$$

where n_0 denotes the original number of hydrogen molecules in the system before the absorption, n_1 is the number of the hydrogen atoms bound to the graphene sheet.

According to the ideal gas law,

$$n_0 - n_1 = \frac{PV}{k_B T} \quad (10)$$

where P , V , T are the hydrogen gas state variables at the current state. In moving to a continuum, n_1 can be related to the concentration $C(x)$ that is the ratio of hydrogen attached graphene atoms to the unattached ones.

(continued on next page)

$$n_1 = \int \Lambda C dx^2 \quad (11)$$

where Λ is the density of atomic sites.

Next, we derive a continuum model of the binding energy ϵ_b based on the results of atomistic computation, given in Ref. 6. It was shown that the total binding energy depends on the number of C-H bonds N_1 (each requiring an energy ϵ_0), the number of unpaired π electrons N_2 (energy ϵ_π) and the number of C-C bonds between hydrogenated graphene atoms and non-hydrogenated graphene atoms, N_3 (energy ϵ_d). The total binding energy is

$$n_1 \epsilon_b = N_1 \epsilon_0 + N_2 \epsilon_\pi + N_3 \epsilon_d \quad (12)$$

For example, with one absorbed hydrogen atom (shown in blue in Fig. 1), Eq. 12 (using the value 0.8eV from Ref. 6) becomes

$$\epsilon_b = \epsilon_0 + \epsilon_\pi + 3\epsilon_d = 0.8\text{eV} \quad (13)$$

With two neighboring sites occupied by H-atoms placed in opposite sides of the graphene layer (Fig. 2), Eq. 12 (using the energy computed in Ref. 6) gives

$$2\epsilon_b = 2\epsilon_0 + 4\epsilon_d = 3.4\text{eV} \quad (14)$$

When three hydrogen atoms absorbed as shown in Fig. 3,

$$3\epsilon_b = 3\epsilon_0 + \epsilon_\pi + 5\epsilon_d = 5.2\text{eV} \quad (15)$$

solving Eq. 13, Eq. 14, and Eq. 15.

$$\epsilon_0 = 2.7\text{eV} \quad \epsilon_\pi = -0.4\text{eV} \quad \epsilon_d = -0.5\text{eV} \quad (16)$$

Note that the energies of all other small clusters computed in Ref. 6 can be evaluated using Eq. 16, and decoupling the interactions into on-site, π bonds and nearest neighbor components. We only consider patches of H-absorption, where there is at most one unpaired π electron. When the number of absorbed H-atoms is large, the contribution of ϵ_π from the unpaired H-atom can be neglected, and Eq. 12 reduces to

$$n_1 \epsilon_b = n_1 \epsilon_0 + N_3 \epsilon_d \quad (17)$$

This equation can be interpreted as follows: the total energy is a sum of an on-site component (ϵ_0) and nearest neighbor energy (ϵ_d). This is our Ising model. Note that using $C = 1$ at occupied sites and $C = 0$ at unoccupied sites, N_3 can be expressed as

$$N_3 = \frac{1}{2} \sum_{i,j} (C_i - C_j) \quad (18)$$

where i and j are neighboring sites. Now we consider large-scale H-absorbed regions and introduce a continuum formulation of the problem, in terms of a concentration field $C(x)$ for absorbed H. For example,

$$n_1 = \int \Lambda C dx^2 \quad (19)$$

In the continuum case, Eq. 18 can be written (assuming isotropy)

$$N_3 = \frac{1}{2} a^2 \Lambda \int (\nabla C)^2 dx^2 \quad (20)$$

It is worth noting that Eq. 20, in a phenomenological sense, incorporates part of the cost of the elastic energy (caused by the deformation due to binding of hydrogen). It can be rationalized that mechanical strain occurs due to the gradient of the concentration field (in other words for a uniform concentration there is no cost in elastic energy). Substituting Eq. 19, Eq. 20 into Eq. 17, gives

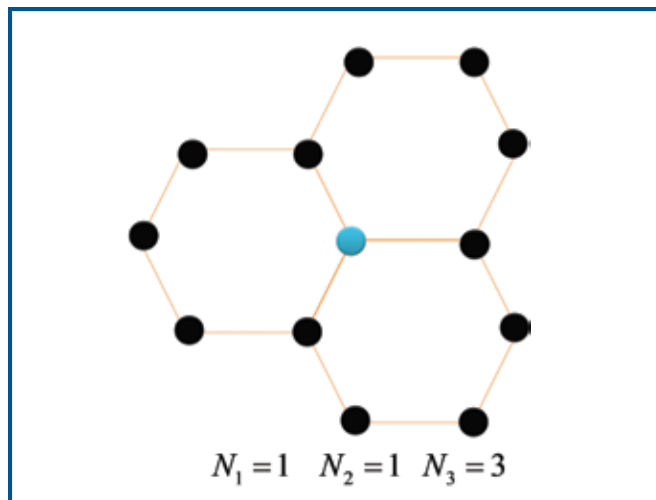


Fig. 1. Schematic diagram of a graphene sheet, one of whose C-atoms has absorbed a H-atom.

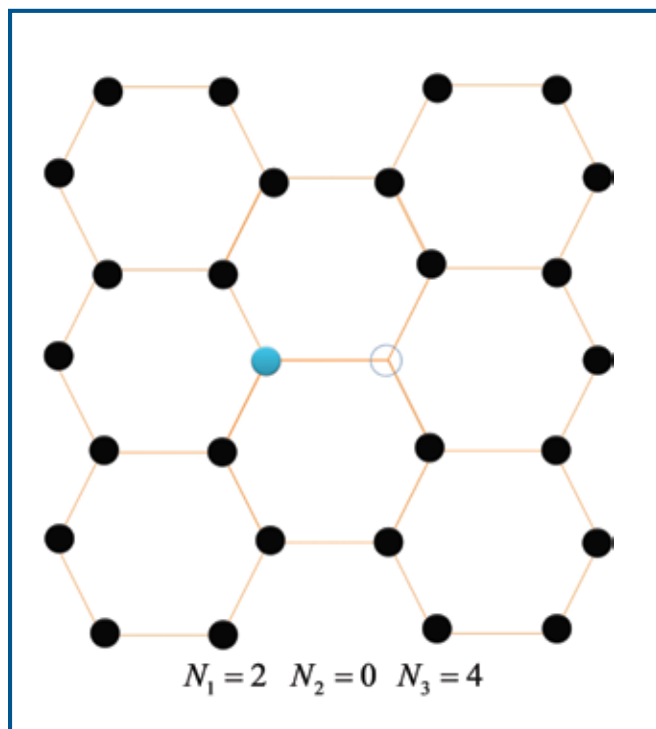


Fig. 2. Schematic diagram of a graphene sheet, where two neighboring C-atoms have absorbed H-atoms. The two H-atoms are on opposite sides of the graphene sheet.

$$n_1 \epsilon_b = \Lambda \epsilon_0 \int C dx^2 + \frac{1}{2} a^2 \Lambda \epsilon_d \int (\nabla C)^2 dx^2 \quad (21)$$

We only need an expression for the entropy of the graphene sheet in order to compute Eq. 6. The entropy is

$$S_g = k_B \ln \Omega \quad (22)$$

where Ω is the number of all the possible microscopic states of the system.

Since neighboring H-atoms are assumed to lie on either side of graphene, all we need to do is to identify $(n/2)$ locations for the H-atoms on one side of the graphene. This is approximately

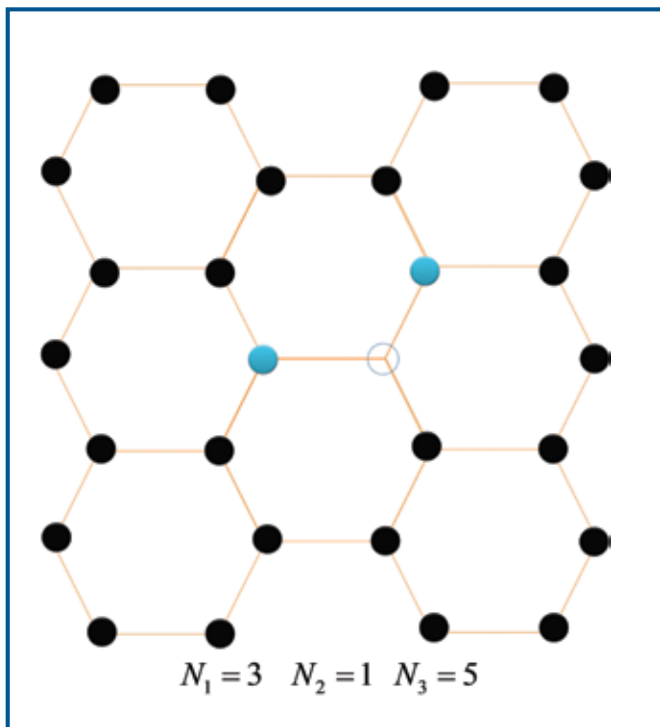


Fig. 3. Schematic diagram of a graphene sheet, with H-absorption in 3 neighboring C-atoms. The solid spheres indicate absorption above the graphene sheet while the open circle indicates absorption below the sheet.

$$\Omega = \frac{\left(\frac{1}{2}n_1\right)!}{\left(\frac{1}{2}n_g\right)! \left(\frac{1}{2}(n_g - n_1)\right)!} \quad (23)$$

where n_g is the total number of the graphene atoms, half of which can be occupied by H-atoms lying on the chosen side of graphene.

Thus,

$$\begin{aligned} S_g &= k_B \ln \Omega \\ &\approx k_B \left[\frac{1}{2}n_g \ln \left(\frac{1}{2}n_g\right) - \frac{1}{2}n_g - \frac{1}{2}n_1 \ln \left(\frac{1}{2}n_1\right) + \frac{1}{2}n_1 \right. \\ &\quad \left. - \frac{1}{2}(n_g - n_1) \ln \left(\frac{1}{2}(n_g - n_1)\right) + \frac{1}{2}(n_g - n_1) \right] \\ &= -\frac{1}{2}k_B \left(n_1 \ln \frac{n_1}{n_g} + (n_g - n_1) \ln \frac{n_g - n_1}{n_g} \right) \end{aligned} \quad (24)$$

Now, Eq. 9 reduces to

$$\begin{aligned} G &= (1 + c_v)k_B(n_0 - n_1)T \\ &\quad - (n_0 - n_1)k_B T \left(\ln T^{\frac{5}{2}} + \ln \frac{V}{n_0 - n_1} + 69.22 \right) \\ &\quad + \Lambda(\varepsilon_{H_2} - \varepsilon_0) \int C dx^2 - \frac{1}{2}a^2 \Lambda \varepsilon_d \int (\nabla C)^2 dx^2 \\ &\quad + \frac{1}{2}k_B T \left(n_1 \ln \frac{n_1}{n_g} + (n_g - n_1) \ln \frac{n_g - n_1}{n_g} \right) \end{aligned} \quad (25)$$

The chemical potential of the system is given by⁷

$$\begin{aligned} \mu &= \frac{\delta G}{\delta C} \\ &= \Lambda \left[\varepsilon_{H_2} - \varepsilon_0 - k_B T \left(c_v + 2 - 69.22 - \ln T^{\frac{5}{2}} - \ln \frac{V}{n_0 - n_1} \right) \right. \\ &\quad \left. + a^2 \varepsilon_d \Delta C + \frac{1}{2}k_B T \ln \frac{n_1}{n_g - n_1} \right] \\ &= \Lambda \left[\varepsilon_{H_2} - \varepsilon_0 - k_B T \left(-64.72 - \ln \frac{k_B T^{\frac{7}{2}}}{P} \right) \right. \\ &\quad \left. + a^2 \varepsilon_d \Delta C + \frac{1}{2}k_B T \ln \frac{n_1}{n_g - n_1} \right] \end{aligned} \quad (26)$$

In our study, we choose a simple gradient system to describe the dynamic behavior of the hydrogen absorption

$$\begin{aligned} \frac{\partial C}{\partial t} &= -\mu \\ &= \Lambda \left[-\varepsilon_{H_2} + \varepsilon_0 - a^2 \varepsilon_d \Delta C - k_B T \left(64.72 + \ln \frac{k_B T^{\frac{7}{2}}}{P} \right) \right. \\ &\quad \left. - \frac{1}{2}k_B T \ln \frac{n_1}{n_g - n_1} \right] \end{aligned} \quad (27)$$

After rescaling time by Λ , Eq. 27 becomes

$$\begin{aligned} \frac{\partial C}{\partial t} &= -\varepsilon_{H_2} + \varepsilon_0 - \varepsilon_d \Delta C - k_B T \left(64.72 + \ln \frac{k_B T^{\frac{7}{2}}}{P} \right) \\ &\quad - \frac{1}{2}k_B T \ln \frac{C_{Avg}}{1 - C_{Avg}} \end{aligned} \quad (28)$$

Now we can integrate the model system to find the equilibrium solutions. One set of conditions is to keep the pressure and the temperature of the ambient gas to be fixed. Under such conditions, either all sites are occupied or vacant. The solid line of Fig. 4 shows the phase boundary between parameters for which hydrogen is absorbed and desorbed from graphene. The corresponding results from atomistic computations have been reported in Ref. 6, and are shown by the dashed line. There is qualitative (and reasonably good quantitative) agreement between the phase boundaries.

The more interesting problem is what happens when the number of H₂ molecules is fixed and the initial pressure is close to the transition line. Then, as the hydrogen is partially absorbed, the external pressure drops below the transition, and the absorption stops. The issue then is what are the patterns of absorption? Figure 5 shows some examples of H-absorbed states.

Concluding Remarks

In conclusion, we have noted that the atomistic computations of hydrogen absorption on graphene agree with a simple Ising type model, and have used this observation to introduce a thermodynamic model for the process, that can be used for computations of H-absorption on a large scale. We used the model system to calculate the phase boundary between graphene and graphene.

(continued on next page)

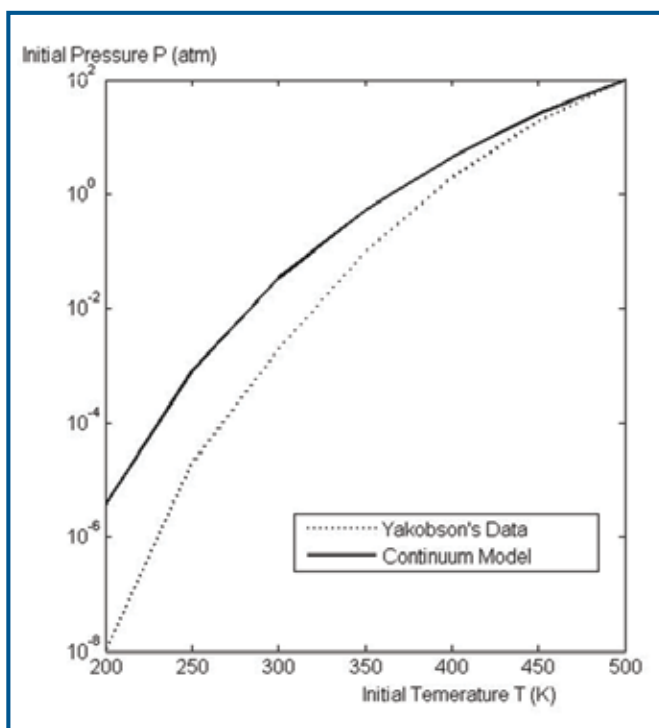


FIG. 4. Thermodynamic equilibrium lines when the initial concentration is 4.8×10^{-8} .

Our model²⁸ does not exhibit bistability, and hence there are no stable graphene/graphene boundaries on a large scale. However, such boundaries were shown to exist in atomistic calculations.⁸ These atomistic calculations did not consider long-wavelength instabilities that can destabilize the interface. We would like to point out that our continuum generalization of the Ising model used the lowest order spatial derivatives. In principle, we could have introduced a continuum model containing higher order derivatives, which would have reduced to the same identical discrete Ising model. The stability of graphene/graphene boundaries may be different in these models. In the absence of experimental results on the stability of domains of graphane in graphene, it is difficult to determine which system best models the experiment.

In our computations, we also assumed that the graphene sheet does not experience crumpling.⁹⁻¹¹ However, suspended graphene sheets are known to exhibit crumpling at a microscopic scale,^{12,13} as can be inferred on general grounds.¹⁴ The computations outlined in the paper will need to be modified to account for such surface roughening.

Our model can be used to calculate long-term dynamics of hydrogen absorption on graphene, and to determine if graphene can be used as a practical means for hydrogen storage for mobile applications. Specifically, Figure 5 can be used to identify external conditions under which hydrogen can absorb or desorb from the graphene sheet.

Recent studies have shown that decoration with metal atoms appears to enhance the hydrogen storage capacity of graphene.⁵ Our thermodynamic approach can be easily extended to these situations as well. All that is needed is the energy of a small number of configurations whose energies are computed from atomistic calculations.

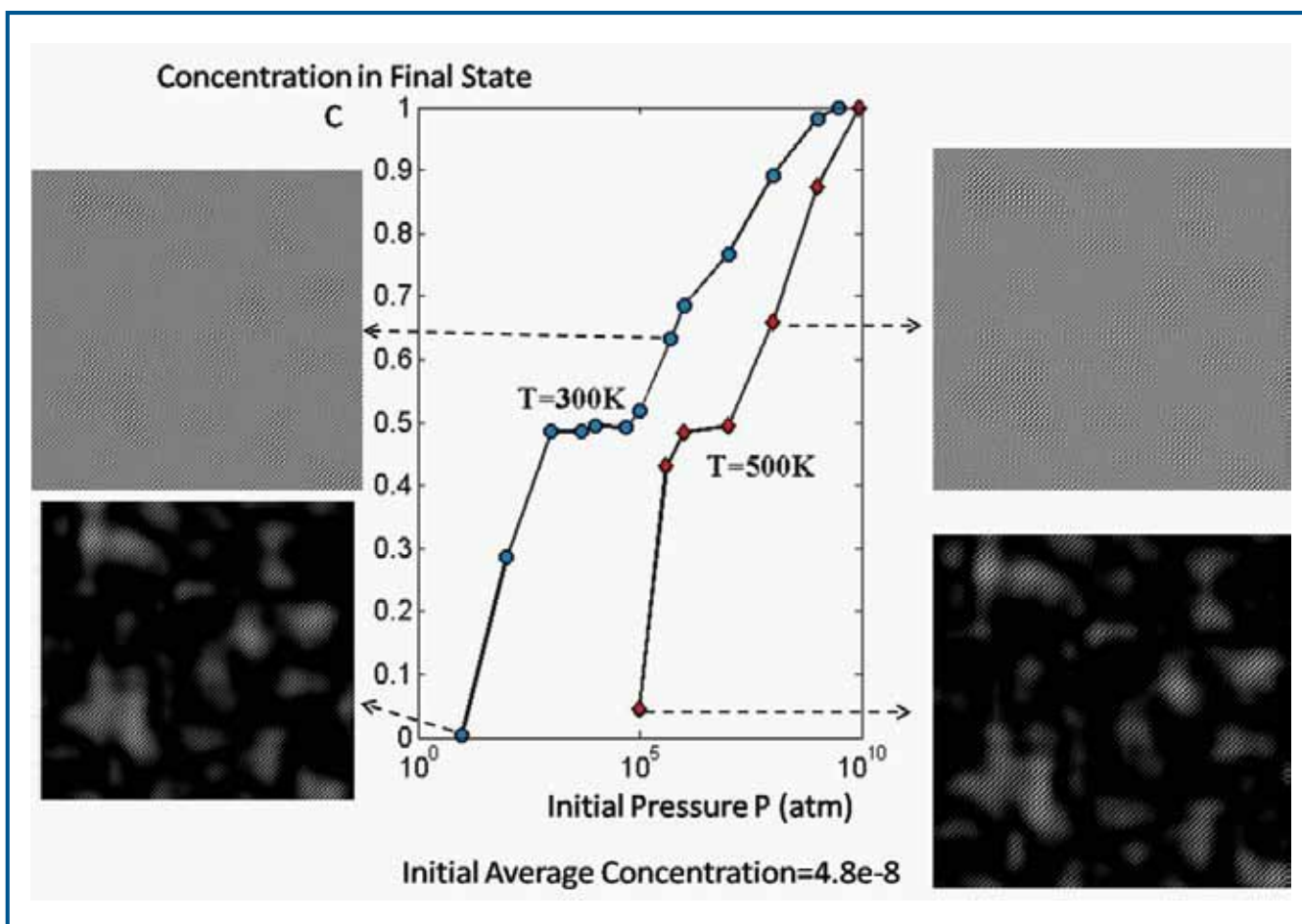


FIG. 5. The maximum loadings that can be reached at different initial pressures.

Acknowledgments

This work was partially funded by the grant CMMI-0709293 from the National Science Foundation and by a grant from the Texas Higher Education Coordinating Board. ■

About the Authors

FENG SHI completed his doctorate degree in mechanical engineering at the University of Houston (2009). He is working as a research engineer in Saint-Gobain Research, Shanghai, China. His current work is focused on theoretical and experimental tribology of polymers. He may be reached at feng.shi@saint-gobain.com.

AMAR BHALLA is a Distinguished Research Professor in the Department of Electrical & Computer Engineering, University of Texas at San Antonio. His current research emphasis leads to the understanding of the overlapping boundaries of nanostructure ferroics and multifunctionality and to exploit their role in developing sensors for structural health and human health monitoring, and their use for energy harvesting. He is a fellow of American Ceramic Society, Fellow of Optical Society of America, and member of several professional societies. He may be reached at amar.bhalla@utsa.edu.

CHONGLIN CHEN is currently a professor in the Department of Physics and Astronomy at the University of Texas at San Antonio and a joint professor at the Texas Center for Superconductivity at the University of Houston (TcSUH). His research interests have spanned over the areas of multifunctional oxide thin film epitaxy, nanostructure fabrication, surface and interface physics and chemistry, and modeling developments. He may be reached at cl.chen@utsa.edu.

GEMUNU H. GUNARATNE is a professor and the Associate Chair of the Department of Physics at the University of Houston. His research interests include pattern formation, nanostructures, biological networks, and quantitative analysis of financial markets. He may be reached at gemunu@uh.edu.

JIECHAO JIANG is a research associate professor in the Materials Science and Engineering Department at the University of Texas at Arlington (UTA). He is the Facility Manager of UTA Characterization Center for Materials and Biology. His research interests include microstructures and defects of advanced materials and their processing-microstructure-property relationship, nucleation, growth mechanisms, interface structures and surface morphologies, structural modeling and simulation of epitaxial thin films. He may be reached at jiang@uta.edu.

EPISTATHIOS "STATHIS" I. MELETIS is a professor and Chair of the Materials Science and Engineering Department at the University of Texas at Arlington (UTA). He previously held appointments at Louisiana State University (as an Endowed Chair Professor), University of California Davis, IITRI, and Georgia Tech and has been a recipient of William Fulbright Research Award. He is the Editor-in-Chief of the *Journal of Nano Research*. His current research interests include: basic processing-structure-property relationships in small-scale materials (nanomaterials, multifunctional and functionally gradient nanomaterials, self-organization, nanofabrication, surface layers, thin films, and coatings), and material-environment interactions. He may be reached at meletis@uta.edu.

References

1. A. K. Geim and K. S. Novoselov, *Nature Mater.*, **6**, 183 (2007).
2. S. Das Sarma, A. K. Geim, P. Kim, and A. H. MacDonald, Eds., Special Edition: Exploring Graphene-Recent Research Advances, *Solid State Commun.* **143**, Issues 1-2 (2007).
3. A. H. Castro Neto, F. Guinea, N. M. R. Perez, K. S. Novoselov, and A. K. Geim, *Rev. Mod. Phys.*, **81**, 109 (2009).
4. A. K. Geim, *Science*, **324**, 1530 (2009).
5. H. Lee, J. Ihms, M. L. Cohen, and S. G. Louie, *Nano Lett.*, **10**, 793 (2010).
6. Y. Liu, F. Ding, and B. I. Yakobson, *Phys. Rev. B*, **78**, 041402 (2008).
7. J. B. Ott and J. Beoro-Goates, *Chemical Thermodynamics: Principles and Applications*, Academic Press, California (2000).
8. L. A. Openov and A. I. Podlivaev, *JETP Letters*, **90**, 459 (2009).
9. D. R. Nelson and L. Peliti, *J. Physique*, **48**, 1085 (1987).
10. J. Aronovitz, L. Golubovic, and T. C. Lubensky, *J. Phys.*, **50**, 609 (1989).
11. J. H. Los, M. I. Katsnelson, O. V. Yazyev, K. V. Zakharchenko, and A. Fasolino, *Phys. Rev. B*, **80**, 121405 R (2009).
12. J. C. Meyer, A. K. Geim, M. I. Katsnelson, K. S. Novoselov, T. J. Booth, and S. Roth, *Nature*, **446**, 60 (2007).
13. A. Fasolino, J. H. Los, and M. I. Katsnelson, *Nature Mater.*, **6**, 858 (2007).
14. N. D. Mermin and H. Wagner, *Phys. Rev. Lett.*, **17**, 1133 (1966).